Supplementary Methods:

Synthesis of N-succinimidylpentynoate (NSP) ((2,5-dioxopyrrolidin-1-yl) pent-4-ynoate).

Pentynoic acid (250 mg, 2.55 mmol, Sigma-Aldrich) was dissolved in dry acetonitrile (7.5 ml) and dry pyridine (7.5 ml) under argon atmosphere. After addition of TSTU (*N*,*N*,*N′*,*N′*-tetramethyl-*O*-(*N*-succinimidyl) uroniumtetrafluoroborate, 1.30 g, 4.33 mmol, Molekula) the reaction mixture was stirred for two hours and then taken to dryness via rotary evaporation. The crude product was dissolved in 15 ml chloroform and filtered to remove tetramethylurea. The filtrate was extracted two times with 15 ml of a 1:1 mixture of 0.1 M phosphoric acid and brine and once with 10 ml of brine. The chloroform phase was dried with sodium sulfate and the solvent was evaporated. Yield: 410 mg (2.1 mmol, 82 %). ^{1}H-NMR (300 MHz, CDCl3) δ (ppm): 2.05 (1 H, t, J = 2.5 Hz, ***H***-C≡C-), 2.62 (2 H, dt, J_1 = 7.5 Hz, J_2 = 2.4 Hz, C≡CC***H***2), 2.84 (4 H, s, NHS (*N*-hydroxysuccinimide)), 2.88 (2 H, t, J = 7.5 Hz, -C***H2***-COO-NHS).

Synthesis of CIT-pentynamide (N-[[1-[3-(dimethylamino)propyl]-1-(4-fluorophenyl)-3H-isobenzofuran-5-yl]methyl]pent-4-ynamide).

R- and S-3-(5-(Aminomethyl)-1-(4-fluorophenyl)-1,3-dihydroisobenzofuran-1-yl)-N,N-dimethylpropan-1-amine (CIT-NH_2) were prepared according to a recently published procedure[19]. NSP (3.3 mg, 17 µmol) was dissolved in 200 µl pyridine under argon atmosphere. CIT-NH_2, (5.9 mg, 10 µmol, of the R-enantiomer or 5.4 mg, 10 µmol, of the S-enantiomer, with different molecular weights due to variable contents of oxalate and water) and DIEA (*N*,*N*-diisopropylethylamine, 5 µl, 30 µmol, Sigma-Aldrich) were added and the mixture was stirred for 3 h. Subsequently, water (20 µl) was added and the reaction mixture stirred for 1 h at 35 °C to allow for hydrolysis of the excess NSP. The mixture was diluted with 5 ml of toluene and taken to dryness via rotary evaporation. The residue was dissolved in 10 ml chloroform and washed twice with a mixture of 1 ml 10 % Na_2CO_3 and 1 ml brine, then once with 2 ml brine. The chloroform phase was dried over sodium sulfate and the solvent removed via rotary evaporation. Yield: 3.0 mg (7.3 µmol, 73 %) of S-CIT-pentyne and 3.9 mg (9.5 µmol, 95 %) of R-CIT-pentyne. ^{1}H-NMR (300 MHz) δ (ppm): 1.37-1.54 (2 H, m, C***H₂***-CH_2-N-$(CH_3)_2$), 1.98 (1 H, t, J = 2.6 Hz, C≡C***H***), 2.08-2.16 (8 H, m, C***H₂***-CH_2-CH_2-N-(C***H₃***)$_2$), 2.25 (2 H, t, J = 7.3 Hz, C***H₂***-N-$(CH_3)_2$), 2.43 (2 H, t, J = 6.8 Hz, C***H₂***-CON-CIT), 2.56 (2 H, m, HC≡C-C***H₂***), 4.45 (2 H, d, J =

5.8 Hz, pentyne-CON-C***H₂***), 5.12 (2 H, d, J = 2.7 Hz, C***H₂***-O cyclic), 6.97 (2 H, t, J = 8.7 Hz, aromatic), 7.14 (1 H, s, aromatic), 7.17-7.26 (2 H, m, aromatic), 7.40-7.48 (2 H, m, aromatic).

Synthesis of HO-glu-PEG$_{20}$-N$_3$ (1-azido-61-oxo-3, 6, 9, 12, 15, 18, 21, 24, 27, 30, 33, 36, 39, 42, 45, 48, 51, 54, 57, 60-icosaoxapentahexacontan-65-oic acid).

HO-PEG$_{20}$-N$_3$ (59-azido-3,6,9,12,15,18,21,24,27,30,33,36,39,42,45,48,51,54,57-nonadecaoxanonapentacontan-1-ol, 100 mg, 108 µmol, Polypure,) was dissolved in 1 ml dry pyridine under argon atmosphere. After addition of glutaric anhydride (57 mg, 500 µmol, Sigma-Aldrich) and TEA (*N*,*N*,*N*-triethylamine, 104 µl, 750 µmol, Sigma-Aldrich), the reaction mixture was stirred over night at 35-37 °C. Excess glutaric anhydride was hydrolyzed by adding 100 µl H_2O and stirring for 2 h at 35–37 °C. The reaction mixture was diluted with 15 ml of toluene and taken to dryness via rotary evaporation. The precipitate was dissolved in 15 ml chloroform and extracted with 0.1 M phosphoric acid and brine. The chloroform phase was dried using sodium sulfate and taken to dryness via rotary evaporation. Yield: 102 mg (98 µmol, 91 %). ^{1}H-NMR (300 MHz, $CDCl_3$) δ (ppm): 1.97 (2 H, m, CH_2-C***H₂***-CH_2-COOH), 2.36-2.46 (4 H, m, C***H₂***-CH_2-C***H₂***-COOH), 3.39 (2 H, t, J = 5.0 Hz, C***H₂***-N_3), 3.57-3.71 (76 H, broad s, C***H₂***-O-C***H₂***), 4.25 (2 H, t, J = 4.6 Hz, C***H₂***-O-glu).

Synthesis of NHS-glu-O-PEG$_{20}$-N$_3$ (59-azido-3, 6, 9, 12, 15, 18, 21, 24, 27, 30, 33, 36, 39, 42, 45, 48, 51, 54, 57-nonadecaoxanonapentacontyl (2,5-dioxopyrrolidin-1-yl) glutarate).

HO-glu-PEG$_{20}$-N$_3$ (100 mg, 96 µmol) was dissolved in 500 µl dry acetonitrile and 500 µl dry pyridine under an argon atmosphere. TSTU (49 mg, 163 µmol) was added and the mixture was stirred for 2 h. Ten ml toluene was added and the solvents were evaporated. The residue was dissolved in 15 ml chloroform, insoluble material (excess of TSTU) was filtered off. The filtrate was washed two times with 10 ml of a 1:1 mixture of 0.1 M NaH_2PO_4 and brine and once with 10 ml brine, dried over sodium sulfate and taken to dryness via rotary evaporation. Yield: 81 mg (71 µmol, 74 %). ^{1}H-NMR (300 MHz, $CDCl_3$) δ (ppm): 2.02-2.12 (2 H, m, CH_2-C***H₂***-CH_2-COO-NHS), 2.50 (2 H, t, J = 7.2 Hz, C***H₂***-CH_2-CH_2-COO-NHS), 2.72 (2 H, t, J = 7.3 Hz, C***H₂***-COO-NHS), 2.84 (4 H, s, NHS), 3.39 (2 H, t, J = 5.2 Hz, C***H₂***-N_3), 3.56-3.72 (76 H, broad s, C***H₂***-O-C***H₂***), 4.25 (2 H, t, J = 4.8 Hz, C***H₂***-O-glu).

Synthesis of HO-glu-PEG$_8$-N$_3$ (1-azido-25-oxo-3,6,9,12,15,18,21,24-octaoxanonacosan-29-oic acid).

HO-PEG$_8$-N$_3$ (23-azido-3,6,9,12,15,18,21-heptaoxatricosan-1-ol, 198 mg, 500 µmol, Polypure) was dissolved in 2.5 ml dry pyridine under argon atmosphere. After addition of glutaric anhydride 228 mg, 2000 µmol, Sigma-Aldrich) and TEA (*N*,*N*,*N*-triethylamine, 418 µl, 3000 µmol, Sigma-Aldrich) the reaction mixture was stirred over night at 35-37 °C. Excess glutaric anhydride was hydrolyzed by adding 250 µl H_2O and stirring for 2 h at 35–37 °C. The reaction mixture was diluted with 15 ml of toluene and taken to dryness via rotary evaporation. The precipitate was dissolved in 15 ml chloroform and extracted with 0.1 M phosphoric acid and brine. The chloroform phase was dried using sodium sulfate and taken to dryness via rotary evaporation. Yield: 215 mg (420 µmol, 84 %). ^{1}H-NMR (300 MHz, $CDCl_3$) δ (ppm): 1.97 (2 H, m, CH_2-C***H*****$_2$**-CH_2-COOH), 2.36-2.46 (4 H, m, C***H*****$_2$**-CH_2-C***H*****$_2$**-COOH), 3.40 (2 H, t, J = 5.0 Hz, C***H*****$_2$**-N_3), 3.59-3.73 (28 H, broad s, C***H*****$_2$**-O-C***H*****$_2$**), 4.25 (2 H, t, J = 4.6 Hz, C***H*****$_2$**-O-glu).

Synthesis of NHS-glu-PEG$_8$-N$_3$ (23-azido-3,6,9,12,15,18,21-heptaoxatricosyl (2,5-dioxopyrrolidin-1-yl) glutarate).

HO-glu-PEG$_8$-N$_3$ (1-azido-25-oxo-3,6,9,12,15,18,21,24-octaoxanonacosan-29-oic acid, 51 mg, 100 µmol) was dissolved in 500 µl dry acetonitrile and 500 µl pyridine under argon atmosphere. TSTU (60 mg, 200 µmol) was added and the mixture was stirred over night. After addition of 10 ml toluene, the solution was taken to dryness via rotary evaporation. The residue was dissolved in 15 ml chloroform, insoluble material (excess of TSTU) was filtered off. The filtrate was washed two times with 10 ml of a 1:1 mixture of 0.1 M NaH_2PO_4 and brine, then once with 10 ml brine and dried over sodium sulfate. The solvent was removed via rotary evaporation. Yield: 49 mg (80.7 µmol, 81 %). ^{1}H-NMR (300 MHz, $CDCl_3$) δ (ppm): 2.07 (2 H, t, J = 7.2 Hz, C***H*****$_2$**-CH_2-COOH-NHS), 2.44 (2 H, t, J = 6.9 Hz, C***H*****$_2$**-CH_2-CH_2-COO-NHS), 2.72 (2 H, t, J = 7.2 Hz, C***H*****$_2$**-COO-NHS), 2.83 (4 H, s, NHS), 3.39 (2 H, t, J = 5.1 Hz, C***H*****$_2$**-N_3), 3.60-3.73 (28 H, broad s, C***H*****$_2$**-O-CH_2), 4.2 (2 H, m, C***H*****$_2$**-O-glu-NHS)

Synthesis of N_3-PEG_8-glu-CIT (23-azido-3,6,9,12,15,18,21-heptaoxatricosyl 5-(((1-(3-(dimethylamino)propyl)-1-(4-fluorophenyl)-1,3-dihydroisobenzofuran-5-yl)methyl)amino)-5-oxopentanoate).

NHS-glu-O-PEG_8-N_3 (20 mg, 20 µmol) was dissolved in 100 µl pyridine under argon atmosphere. CIT-NH_2, (5.9 mg, 10 µmol, of the R-enantiomer or 5.4 mg, 10 µmol, of the S-enantiomer, with different molecular weights due to variable contents of oxalate and water) and DIEA (*N*,*N*-diisopropylethylamine, 17 µl, 100 µmol, Sigma-Aldrich) were added and the mixture was stirred over night. Subsequently, water (20 µl) was added and the reaction mixture stirred for 1 h at 35 °C to allow for hydrolysis of the excess NHS-glu-O-PEG_8-N_3. The mixture was diluted with 5 ml of toluene and taken to dryness via rotary evaporation. The residue was dissolved in 10 ml chloroform and washed twice with a mixture of 5 ml 10 % Na_2CO_3 and 5 ml brine, then once with 2 ml brine. The chloroform phase was dried over sodium sulfate and the solvent removed via rotary evaporation. Yield: 5.6 mg (6.8 µmol, 68 %) of N_3-PEG_8-O-glu-SCIT and 5.8 mg (7.1 µmol, 71 %) of N_3-PEG_8-O-glu-RCIT. ^{1}H-NMR (300 MHz) δ (ppm): 1.39-1.53 (2 H, m, C***H₂***-CH_2-N-$(CH_3)_2$), 1.97 (2 H, m, C***H₂***-CH_2-CO-CIT) 2.08-2.16 (8 H, m, C***H₂***-CH_2-CH_2-N-(C***H₃***)$_2$), 2.19-2.31 (4 H, m, C***H₂***-N-$(CH_3)_2$ and C***H₂***-CO-CIT), 2.39 (2 H, m, CO-C***H₂***-CH_2-CH_2-CO-CIT), 3.39 (2 H, t, J = 4.9 Hz, C***H₂***-N_3), 3.51-3.73 (28 H, broad s, C***H₂***-O-CH_2), 4.42 (2 H, d, J = 5.8 Hz, PEG-O-glu-CO-C***H₂***), 5.12 (2 H, d, J = 3.4 Hz, C***H₂***-O cyclic), 6.97 (2 H, t, J = 8.7 Hz, aromatic), 7.14 (1 H, s, aromatic), 7.17-7.26 (2 H, m, aromatic), 7.40-7.48 (2 H, m, aromatic).

Functionalization of AFM tips.

AFM cantilever tips (Si_3N_4/MSCT and Si/MSNL, Bruker) were washed in chloroform 3 times (5 min each), dried, washed in acidic piranha solution (3 ml H_2O_2 and 7 ml H_2SO_4) for 30 min, rinsed thoroughly with Millipore water, and dried by heating to 160°C for 10 min. The cleaned cantilevers were amino-functionalized using the gas phase method for reaction with APTES ((3-Aminopropyl)triethoxysilane)[23,24]. Afterwards, the cantilevers were pegylated[25] by incubation for 2 h in 0.5 ml chloroform containing 1 mg NHS-glu-O-PEG_{20}-N_3 and ~1.5% triethylamine, resulting in acylation of the surface-bound amino groups (supplementary Fig.1, a). After rinsing with chloroform and drying, the alkyne-modified citalopram analogue was coupled to the azido-terminated PEGs via co-catalyst-accelerated copper(I)-catalyzed azide-alkyne cycloaddition. The highly water-soluble bathophenanthrolinedisulfonic acid was chosen as co-catalyst[26]. It works best at a pH of 8.5 and may

be used at concentrations equal to, or up to twice the concentration of Cu(I)[26]. Co-catalyst-accelerated copper(I)-catalyzed azide-alkyne cycloaddition is a particularly favourable reaction mechanism that allows small molecule tip-coupling at a concentration of 1 mM (as used here) and even below[26]. The reaction was carried out as follows in an argon-flooded Teflon reaction-chamber. 600 µl 0.5 M Tris (tris-(hydroxymethyl)-aminomethane) in water (pH 8.5 adjusted with HCl), 293 µL DMSO (dimethyl sulfoxide), 2.5 µL 100 mM $CuSO_4$, 25 µL 10 mMbathophenantroleinedisulfonic acid disodium salt trihydrate, 50 µL 20 mM S- or R-enantiomer of CIT-pentynamide in DMSO, and 20 µL 1 M ascorbic acid were mixed in the argon-flooded reaction chamber and degassed by a gentle stream of argon bubbling through the solution via a Pasteur pipette for 1-2 minutes. Finally, 10 µl 2 MNaOH was added to readjust the pH to 8.5. Thus, the final concentrations of Tris, $CuSO_4$, co-catalyst, CIT-pentynamide, ascorbic acid and NaOH were 0.3 M, 0.25 mM, 0.25 mM, 1 mM, 20 mM, and 20 mM, respectively. The cantilevers were incubated in this solution for ~17 h with continuous protection from oxygen by gentle perfusion of the chamber by argon (supplementary Fig.1, b). The cantilevers were washed with phosphate-buffered saline (PBS, PAA) three times and stored in argon-treated PBS at 4 °C.

Cells.

CHOK1 cells were transfected with a human SERT and a SERT mutant (G402H) construct respectively fused with YFP to yield CHOK1-YFP-hSERT and CHOK1-YFP-hSERT-G402H cells. The addition of YFP to the amino terminus of SERT neither alters its substrate nor its inhibitor pharmacology in CHOK1 and HEK293 cells[18,27,28]. Cells were grown on Petri dishes using 1:1 mixture of DMEM (E15-843, high glucose, PAA) and HAM's F12 containing 10% FBS and 0.1% gentamycin. To keep the selection pressure sufficiently high, 0.5% G418 (50 mg/ml) was added to the medium. For AFM measurements, the growth medium was exchanged to a physiological HEPES buffer containing 140 mMNaCl, 5 mMKCl, 1 mM $MgCl_2$, 1 mM $CaCl_2$, and 10 mM HEPES (pH 7.4 with NaOH). For Li^+ buffer, the NaCl was replaced by Li_2CO_3, and the pH was adjusted with HCl.

Uptake Measurement.

CHOK1 cells stably expressing SERT were distributed in 48-well plates (5×10^5 cells). Prior to the experiment, the cells were washed once in uptake buffer (containing 25 mM HEPES, 120 mMNaCl, 5 mMKCl, 1.2 mM $CaCl_2$, and 1.2 mM $MgSO_4$ supplemented with 5 mM D-glucose) and equilibrated

in uptake buffer for 30 min. The cells were then incubated in buffer (0.1 ml) containing either S-CIT, R-CIT, S-CIT-PEG or R-CIT-PEG at a certain concentration respectively. After 5 min, 150 nM tritiated 5-hydroxytryptamine ([^{3}H]5HT, PerkinElmer Life Sciences) was added and uptake was allowed for 1 min at room temperature. Uptake was terminated by removing the buffer and washing the cells with ice-cold buffer. The remaining radioactivity in the cells was determined by liquid scintillation counting[29]. Data are means ± SEM of four to six independent experiments that were carried out in triplicate. Nonspecific uptake in the presence of 10 µM paroxetine was ~10% of total uptake and subtracted. Specific uptake was set 100% to normalize inter-assay variations. The experimental data points were fitted by nonlinear least squares to an equation for the inhibition at a single class of binding sites according to the law of mass action. As shown in supplementary Fig.6, S- and R-CIT-PEG inhibited the uptake of [^{3}H]5HT with an IC_{50} value of 68±11 nM and 1300±130 nM (mean ± SEM), respectively; the IC_{50} values for S- and R-CIT were 2.6±0.4 nM and 128±31 nM, respectively. These measurements indicate that the PEG chain does not block binding of the linked CIT to SERT.

Force-distance curves.

All measurements were carried out at room temperature by using a PicoPlus 5500 AFM setup (Agilent Technologies) on living cells. The S- or R-CIT functionalized cantilever with a nominal spring constant of 0.01 N/m was moved downward to the cell surface and moved upward after the tip touched it. The deflection (z) of the cantilever was monitored by a laser beam on the cantilever surface and plotted *versus* the tip-surface distance, from which the force (F) can be determined according to Hook's law ($F = kz$, with k being the cantilever spring constant). When the tip tethered CIT bound to a SERT on the cell surface, a pulling force developed during the upward movement of the cantilever causing the cantilever to bend downwards. At a critical force, i.e. the unbinding force, the tip tethered CIT detached from SERT, and the cantilever jumped back to its neutral position (supplementary Fig.8). Dynamic force spectroscopy measurements were performed by varying the force loading rate which is the product of the pulling velocity multiplied by the effective spring constant. For this, the sweep range was fixed at 3000 nm, but the sweep rate varied from 0.25 to 2 Hz. For each cellular position and sweep rate, 100-200 force-distance cycles with 2000 data points per cycle and typical force limit of about 30-100 pN were performed. The spring constants of the cantilevers were determined using the thermal noise method[30]. Unbinding forces were determined with an accuracy of 3.1 pN (equivalent to

the cantilever noise). For blocking experiments, 3 mM S- or R-CIT stock solution in DMSO was injected into the 2 mL measurement solution with a final concentration of 30 µM CIT.

Force Data Analysis.

The unbinding event was identified by local maximum analysis using a signal-to-noise threshold of 2. The binding activity was calculated as the fraction of curves showing unbinding events. For example, if 150 curves from 1000 measured curves show unbinding events, the binding activity is 15%. The specificity of the unbinding events was evidenced by performing two control experiments: (i) cantilever tip with PEG linker terminated with azido group but without CIT, measured on CHOK1 cells expressing SERT; (ii) cantilever tips with CIT, measured on CHOK1 cells without SERT. The typical binding activityis 0.78 ± 0.47 (mean ± SEM) for (i) and 1.65 ± 0.34 for (ii), both of which are significantly lower (P< 0.001) than that of any tip with CIT measured on CHOK1 cells expressing SERT. The unbinding force and effective spring constant (slope at rupture) were determined[31] from force curves showing unbinding events. The force loading rate (r) of every individual curve was calculated by multiplying the effective spring constant with the pulling speed. The unbinding force probability density function (PDF) was constructed[32] from every unbinding event on the same cell at the same pulling speed. Unbinding events within the mean force ± standard deviation of the Gaussian fit were used to create an unbinding force *vs.* force loading rate plot for each peak in the force PDF respectively, to show dynamic aspects of the bonds. A maximum likelihood approach[33] was employed to fit the width of the energy barrier x_B and the kinetic off rate k_{off} for the obtained data by using Evans theory[20]. According to the single energy barrier binding model, the probability p that the complex breaks at a certain force, F, is given as [18.33]:

$$p(F) = \frac{k_{off}}{r} \exp\left[\frac{F x_B}{k_B T} - \frac{k_{off} k_B T}{r x_B}\left(exp\frac{F x_B}{k_B T} - 1\right)\right]$$

where k_B is the Boltzmann constant, T is the absolute temperature. The Bayesian information criterion (BIC) was designed to select the best fitting. The formulation for the BIC is given by

$$BIC = -2(l(\psi; y) - l(\psi^*; y)) + 2p\log(\sqrt{n})$$

with $l(\psi;y)$ being the log-likelihood of the model under consideration, $l(\psi^*;y)$ being the log-likelihood of the most likely model in the subset of models considered, p being the number of parameters fit in the

model, and *n* being the number of observations. Two-tailed Student t-test was performed for statistic analysis.

Determination of k_{off} via the whole-cell patch-clamp technique.

Patch-clamp recordings were performed with HEK-293 cells stably expressing hSERT. In all instances, the cells were seeded at low density 24 h before measuring currents. Substrate-induced hSERT currents were recorded under voltage clamp using the whole-cell patch-clamp technique. Glass pipettes contained a solution consisting of 152 mM NaCl, 1 mM $CaCl_2$, 0.7 mM $MgCl_2$, 10 mM EGTA and 10 mM HEPES (pH 7.2 with NaOH) to isolate the substrate-induced peak current. The cells were continuously superfused with external solution (140 mM NaCl, 3 mM KCl, 2.5 mM $CaCl_2$, 2 mM $MgCl_2$, 20 mM glucose and 10 mM HEPES adjusted to pH 7.4 with NaOH). Currents were recorded at room temperature (20-24 °C) using an Axopatch 200B amplifier and pClamp 10.2 software (MDS Analytical Technologies). Cells were voltage clamped to a holding potential 0 mV. Current traces were filtered at 1 kHz and digitized at 2 kHz using a Digidata 1320A (MDS Analytical Technologies). Drugs were applied using a DAD-12 (Adams & List, Westbury, NY, USA), which permits complete solution exchange around the cells within 100 ms. Current amplitudes in response to 5-HT application were quantified using Clampfit 10.2 software. Passive holding currents were subtracted and the traces were filtered using a 100 Hz digital Gaussian low-pass filter.

To assess if pegylation affected CIT binding, we performed electrophysiological measurements of CIT binding to SERT. Upon rapid substrate application, SERT-expressing cells display an inwardly directed peak current[34]. This current can serve as a probe of inhibitor occupancy of SERT because it reads out the fraction of transporters bound by substrate at a given time-point[35]. We employed the following protocol to directly measure k_{off} of CIT (supplementary F**ig.7a**): Application of saturating concentrations of CIT for 5 s reduced the 5-HT-induced peak current, because of occupancy of the binding sites by CIT. Subsequently, the cell was washed, and peak currents were recorded. The longer the cell was washed, the more of the peak current recovered, because more transporters were available for 5-HT binding. The time course of peak current recovery was adequately fit by a mono-exponential function, and yielded k_{off} of CIT (supplementary F**ig.7b, c**). k_{off} R-CIT: 0.34 ± 0.09 s^{-1} *vs.* k_{off} pegylated R-CIT: 0.12 ± 0.01 s^{-1}. Given the slow k_{off} of S-CIT, the electrophysiological approach was not suitable for a thorough characterization of S-CIT binding kinetics. However, it was possible to measure k_{off} of pegylated S-CIT: 0.06 ± 0.01 s^{-1} (supplementary F**ig.7d**).

Supplementary References:

[23] C. K. Riener, *et al.*, *Analytica Chimica Acta* **2003**, *479*, 59-75.

[24] A. Ebner, P. Hinterdorfer, H. J. Gruber, *Ultramicroscopy* **2007**, *107*, 922–992.

[25] L. Wildling, *et al.*, *Bioconjug. Chem.* **2011**, *22*, 1239-1248.

[26] W. G. Lewis, F. G. Magallon, V. V. Fokin, M. G. Finn, *J. Am. Chem. Soc.* **2004**, *126*, 9152-9153.

[27] J. A. Schmid, *et al.*, *J. Biol. Chem.* **2001**, *276*, 3805–3810.

[28] H. Just, H. H. Sitte, J. A. Schmid, M. Freissmuth, O. Kudlacek, *J. Biol. Chem.* **2004**, *279*, 6650–6657.

[29] B. Hilber, *et al.*, *Neuropharmacology* **2005**, *49*, 811–819.

[30] J. L. Hutter, J. Bechhoefer, *Rev. Sci. Instrum.* **1993**, *64*, 1868-1873.

[31] C. Rankl, F. Kienberger, H. Gruber, D. Blaas, P. Hinterdorfer, *Jap. J. Appl. Phys.* **2007**, *46*, 5536–5539.

[32] W. Baumgartner, P. Hinterdorfer, H. Schindler, *Ultramicroscopy* **2000**, *82*, 85-95.

[33] P. Hinterdorfer, A. Oijen (Eds.), Handbook of Single-Molecule Biophysics, Springer (New York), **2009**, A. Ebner, *et.at.*, Ch. *15*, 407-447.

[34] K. Schicker, Z. Uzelac, J. Gesmonde, S. Bulling, T. Stockner, M. Freissmuth, *et al*, *J. Biol. Chem.* **2012**, *287***,** 438-445.

[35] P. S. Hasenhuetl, K. Schicker, X. Koenig, Y. Li, S. Sarker, T. Stockner, *et al*, *Mol. Pharm.* **2015**, *88***,** 12-18.

Supplementary Fig.1

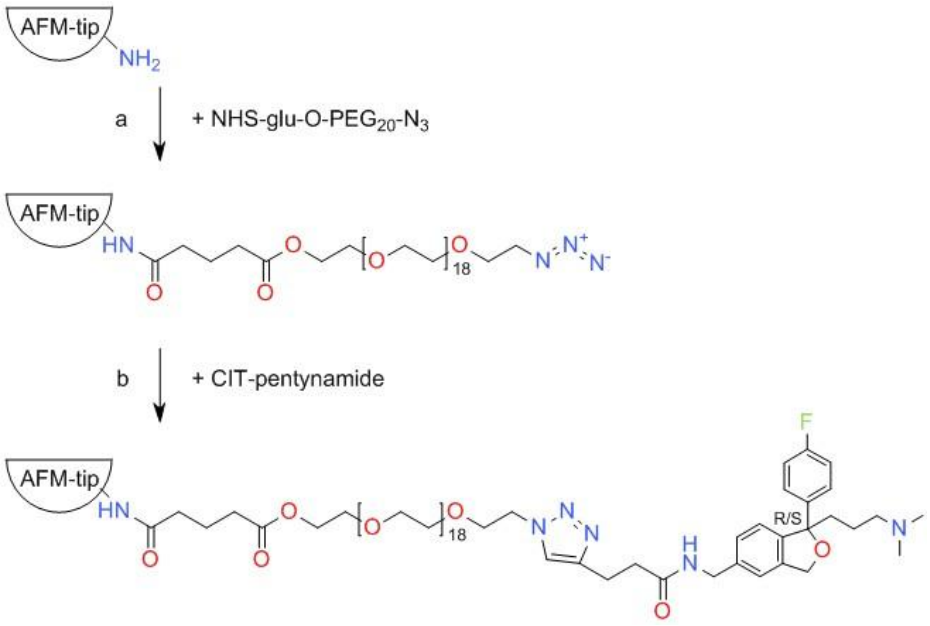

Supplementary Fig.1. Functionalization of the AFM cantilever tip with CIT. The cantilever tip was first amino-functionalized by gas phase reaction with APTES. Subsequently, the NHS-glu-O-PEG_{20}-N_3 linker was conjugated to the surface-bound amino-groups (**a**). The ligand CIT-pentynamide was attached to the linker via azide-alkyne cycloaddition (**b**).

Supplementary Fig.2

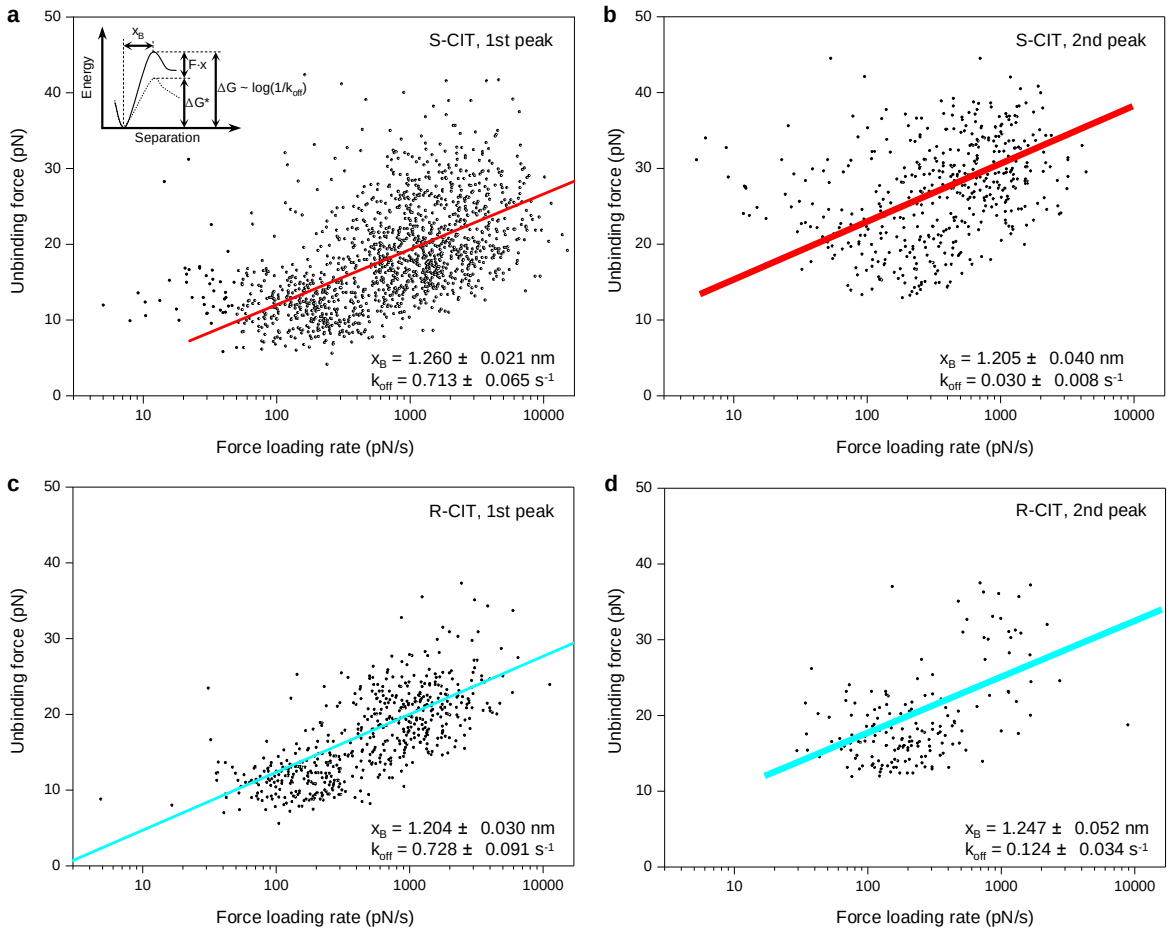

Supplementary Fig.2. Force *vs.* loading rate plots of two populations of unbinding events from S- and R-CIT. Force data points of every unbinding event in the two peaks of the force PDFs were separately plotted against the force loading rate for the S-CIT and R-CIT respectively. The data were fitted with the single energy barrier model, from which the kinetic off rate k_{off} and the width of the energy barrier x_B were extracted. As shown in the inset, ΔG is the energy barrier without force whereas ΔG* is the energy barrier reduced by the applied force (F).

Supplementary Fig.3

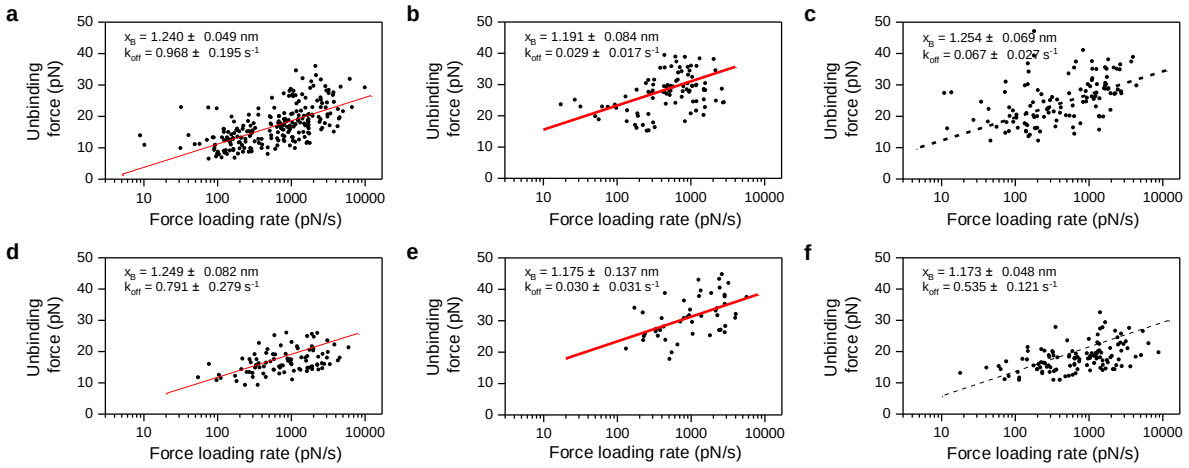

Supplementary Fig.3. Force *vs.* loading rate plots for comparison between wt and mutant and between Na^+ and Li^+ buffer. (**a, d**) wt SERT in Na^+ buffer, 1st peak in force PDF. (**b, e**) wt SERT in Na^+ buffer, 2nd peak. (**c**) SERT-mutant-G402H in Na^+ buffer, using the same cantilever tip as in (**a, b**). (**f**) wt SERT in Li^+ buffer, using the same cantilever tip as in (**d, e**).

Supplementary Fig.4

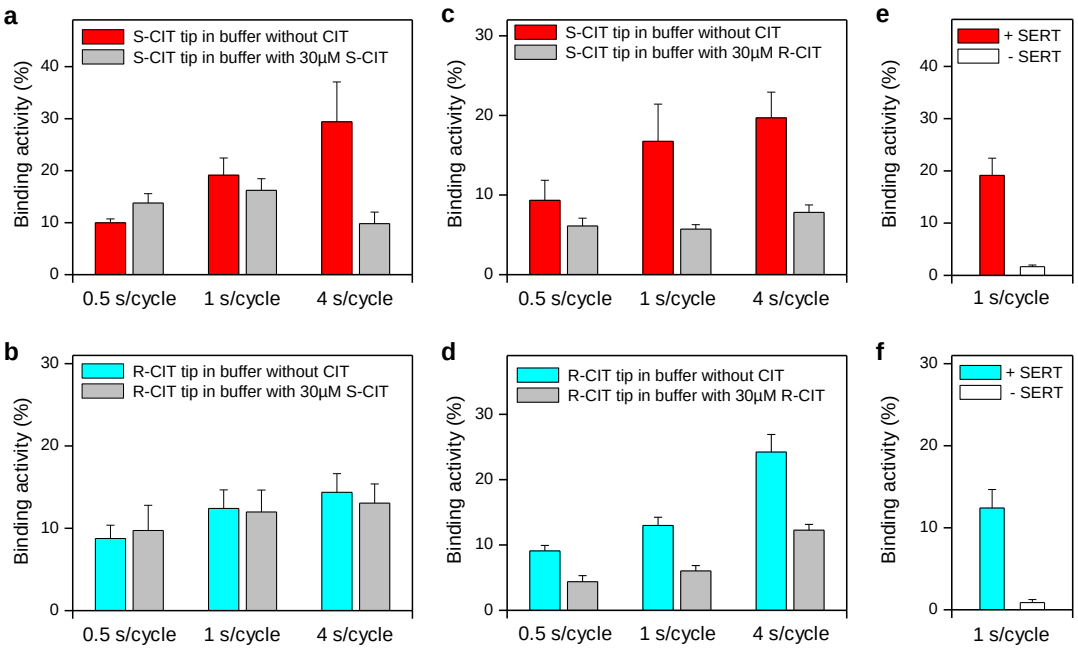

Supplementary Fig.4. Influence of free CIT in buffer solution on the binding activity of tip-linked CIT. Tips functionalized with S-CIT (**a**, **c**) or R-CIT (**b**, **d**) were analyzed on CHOK1-YFP-hSERT cells in buffer solution without CIT with respect to their binding activity. After 30 µM S-CIT (**a**, **b**) or R-CIT (**c**, **d**) was added, the experiments were repeated. Data shown are mean ± SEM. In control experiments on CHOK1 cells lacking SERT(**e** and **f**), the S-CIT and R-CIT tips used in (**a** and **b**) revealed a very low binding activity ($P < 0.001$).

Supplementary Fig.5

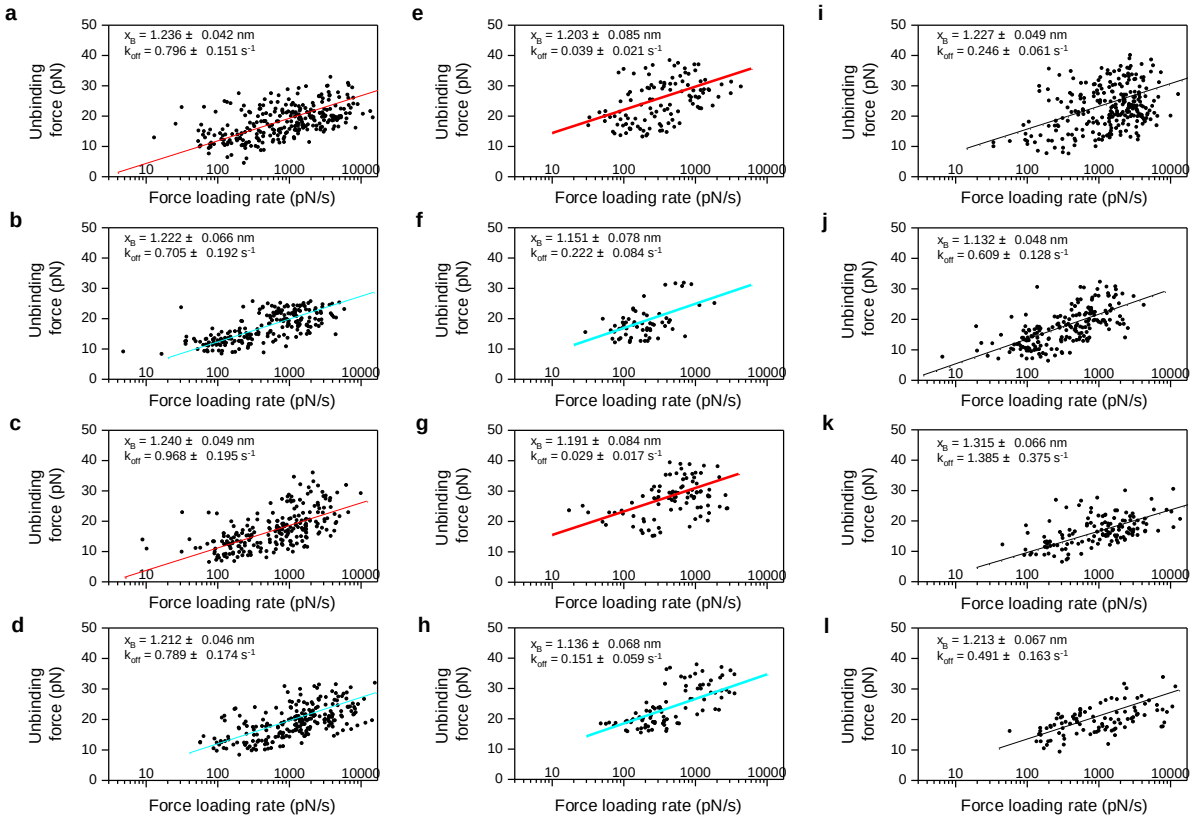

Supplementary Fig.5. Force *vs.* loading rate plots before and after addition of 30 µM CIT. Force data points measured by S-CIT (1st and 3rd row) or R-CIT (2nd and 4th row) tips before (1st column for 1st peak in force PDF; 2nd column for 2nd peak) and after (3rd column) injection of 30 µM S-CIT (1st and 2nd row) or R-CIT (3rd and 4th row) respectively into the measurement solution were plotted against the force loading rate. The data were fitted with the single energy barrier model, from which the kinetic off rate k_{off} and the width of the energy barrier x_B were extracted.

Supplementary Fig.6

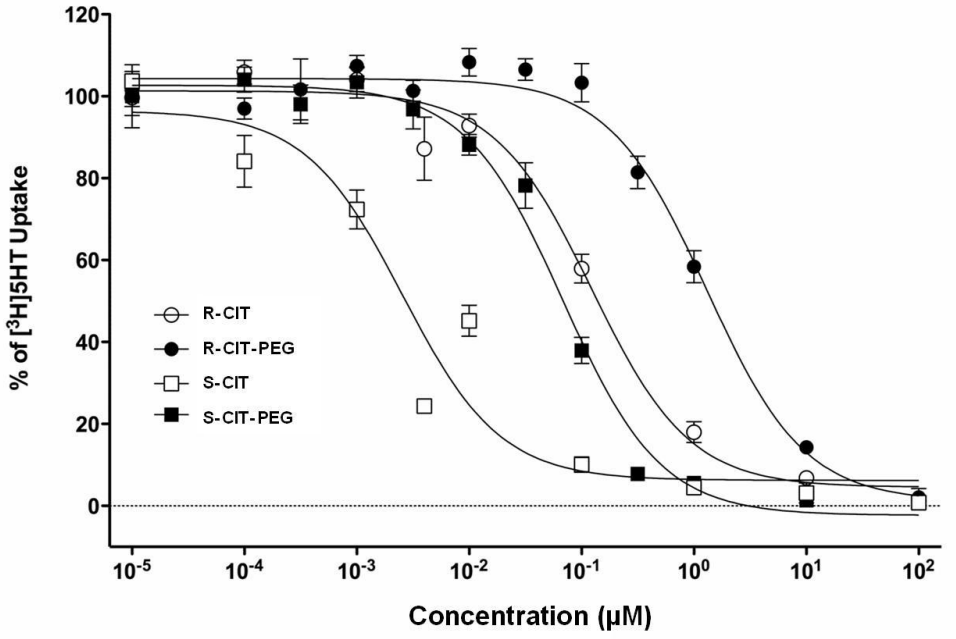

Supplementary Fig.6. Uptake inhibition experiments. CHOK1 cells stably expressing SERT were preincubated in buffer containing either S-CIT, R-CIT, S-CIT-PEG, or R-CIT-PEG at the concentration indicated. After 5 min, [^{3}H]5HT (150 nM) was added and uptake was allowed for 1 min at room temperature and then washed with ice-cold buffer. Radioactivity data are means ± SEM of four to six independent experiments in triplicate. The estimated IC50 value were 2.6±0.4 nM for S-CIT (n=6), 128±31 nM for R-CIT (n=5), 68±11 nM for S-CIT-PEG (n=4), and 1300±130 nM for R-CIT-PEG (n=4), respectively. The measurements indicated that the PEG chain does not block binding of the linked CIT to SERT.

Supplementary Fig.7

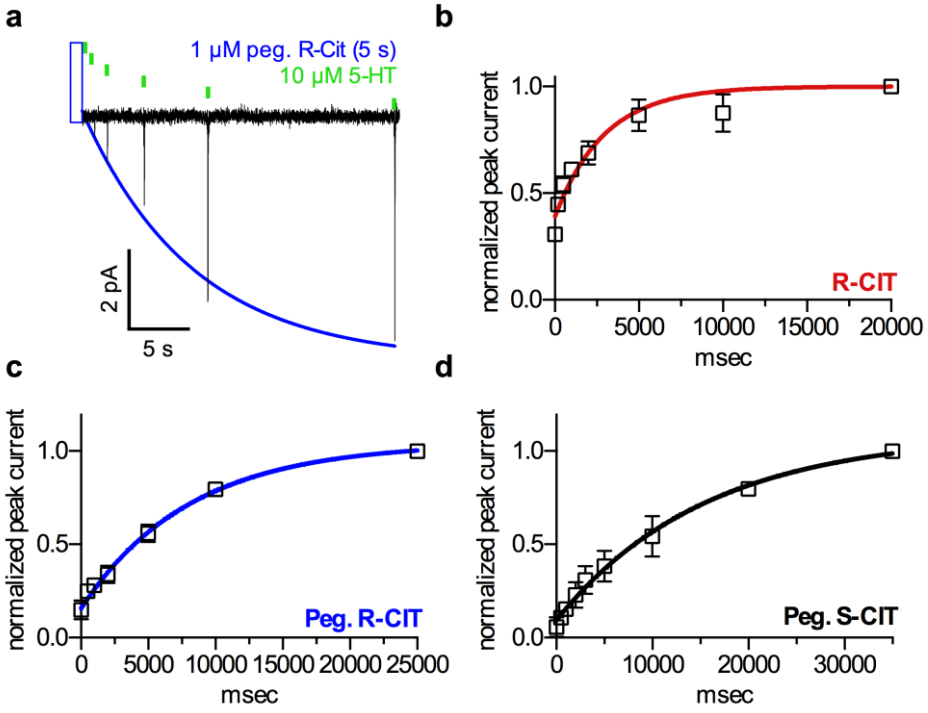

Supplementary Fig.7. k_{off} of R-CIT, pegylated R-CIT, and pegylated S-CIT determined by whole-cell patch-clamp. (**a**) Protocol and time course of peak-current recovery. (**b-d**) Direct measurement of k_{off} of R-CIT, pegylated R-CIT, and pegylated S-CIT, respectively. The time course of peak current recovery can be adequately fit by a mono-exponential function, and yields k_{off}. Data are means ± S.D from 4-8 independent measurements.

Supplementary Fig.8

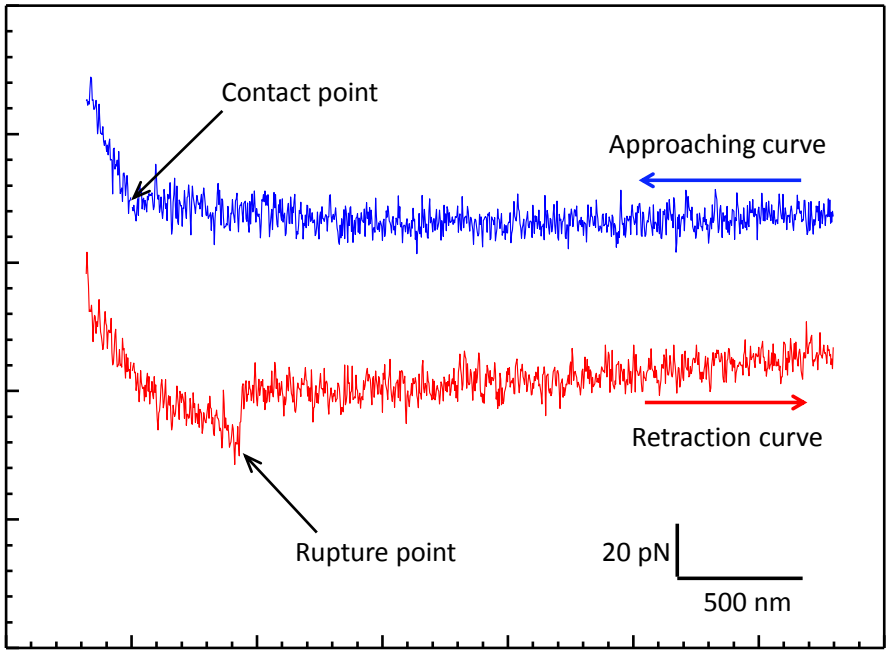

Supplementary Fig.8. Example of full force-distance curves. During approaching (upper curve), the distance between the cantilever tip and the cell surface decreases. At the contact point, the tip touches the cell membrane. After the contact (left side of the contact point), the tip presses gently on the cell membrane. When the force limit (which is about 40 pN here) is reached, the tip retracts from the cell surface. If the CIT binds with the SERT, the cantilever tip is pulled downwards (lower curve) until the two molecules are separated at the rupture point. After the rupture, the cantilever recovers to its resting state. If there is no binding between CIT and SERT during the contact, the retraction curve looks similar to the approaching curve.

Supplementary Table 1. Kinetic off-rate k_{off} and width of energy barrier x_B extracted from force *vs.* loading rate plot.

Sample	k_{off} (s^{-1})	x_B (nm)
(Fig. 2c) wt SERT, Na^+, S-CIT tips (n=6), 1st peak	0.713 ± 0.065	1.260 ± 0.021
(Fig. 2c) wt SERT, Na^+, S-CIT tips (n=6), 2nd peak	0.030 ± 0.008	1.205 ± 0.040
(Fig. 2c) wt SERT, Na^+, R-CIT tips (n=4), 1st peak	0.728 ± 0.091	1.204 ± 0.030
(Fig. 2c) wt SERT, Na^+, R-CIT tips (n=4), 2nd peak	0.124 ± 0.034	1.247 ± 0.052
(Fig. 2f) wt SERT, Na^+, S-CIT tip, 1st peak	0.968 ± 0.195	1.240 ± 0.049
(Fig. 2f) wt SERT, Na^+, S-CIT tip, 2nd peak	0.029 ± 0.017	1.191 ± 0.084
(Fig. 2f) SERT mutant G402H, Na^+, S-CIT tip	0.067 ± 0.027	1.254 ± 0.069
(Fig. 2g) wt SERT, Na^+, S-CIT tip, 1st peak	0.791 ± 0.279	1.249 ± 0.082
(Fig. 2g) wt SERT, Na^+, S-CIT tip, 2nd peak	0.030 ± 0.031	1.175 ± 0.137
(Fig. 2g) wt SERT, Li^+, S-CIT tip	0.535 ± 0.121	1.173 ± 0.048
(Fig. 3e) wt SERT, Na^+, S-CIT tip, 1st peak	0.796 ± 0.151	1.236 ±0.042
(Fig. 3e) wt SERT, Na^+, S-CIT tip, 2nd peak	0.039 ± 0.021	1.203 ±0.085
(Fig. 3e) wt SERT, Na^+, S-CIT tip, 30 µM S-CIT in solution	0.246 ± 0.061	1.227 ± 0.049
(Fig. 3f) wt SERT, Na^+, R-CIT tip, 1st peak	0.705 ± 0.192	1.222 ±0.066
(Fig. 3f) wt SERT, Na^+, R-CIT tip, 2nd peak	0.222 ± 0.084	1.151 ±0.078
(Fig. 3f) wt SERT, Na^+, R-CIT tip, 30 µM S-CIT in solution	0.609 ± 0.128	1.132 ± 0.048
(Fig. 3g) wt SERT, Na^+, S-CIT tip, 1st peak	0.968 ± 0.195	1.240 ±0.049
(Fig. 3g) wt SERT, Na^+, S-CIT tip, 2nd peak	0.029 ± 0.017	1.191 ±0.084
(Fig. 3g) wt SERT, Na^+, S-CIT tip, 30 µM R-CIT in solution	1.385 ± 0.375	1.315 ± 0.066
(Fig. 3h) wt SERT, Na^+, R-CIT tip, 1st peak	0.789 ± 0.174	1.212 ±0.046
(Fig. 3h) wt SERT, Na^+, R-CIT tip, 2nd peak	0.151 ± 0.059	1.136 ±0.068
(Fig. 3h) wt SERT, Na^+, R-CIT tip, 30 µM R-CIT in solution	0.491 ± 0.163	1.213 ± 0.067

Supplementary Table 2. Comparison of kinetic off-rate k_{off} (s^{-1}) measured with electrophysiological method and force spectroscopy method.

	PEG-S-citalopram		**PEG-R-citalopram**	
	S1 site	S2 site	S1 site	S2 site
Electrophysiological method	0.064 [± 0.01 s^{-1}]		0.124 [± 0.01 s^{-1}]	
Force spectroscopy method	0.032 [± 0.005 s^{-1}]	0.817 [± 0.108 s^{-1}]	0.166 [± 0.051 s^{-1}]	0.741 [± 0.043 s^{-1}]